MANUFACTURING OF LIGHTWEIGHT SANDWICH FOAM WITH OPTIMIZED BENDING PROPERTIES FOR INTERIOR AIRCRAFT APPLICATION

M. Salmins, P. Mitschang
Leibniz-Institut für Verbundwerkstoffe, Erwin-Schrödinger-Straße 58, 67663 Kaiserslautern, Deutschland

Abstract

Thermoplastic foams, made from polyetherimide (PEI) for example, combine low densities with excellent flame retardant properties. Therefore, they provide an excellent choice for interior application in commercial aircrafts. However, reduced densities cause low mechanical properties. Structural foams have a sandwich-like structure with a dense surface and low-density foam core. They show increased mechanical properties compared to thermoplastic foams and low part weights compared to solid parts. Thermoplastic foams can be transformed into structural foams by using hot press processes. In such a process, polymer skins are produced on the foam surface through compaction of foam cells at temperatures above glass transition temperature of the amorphous polymer. This paper will present a new process to manufacture structural foams from thermoplastic foams and investigate the effect of this transformation on mechanical properties.

1. INTRODUCTION

State of the art cabin parts, such as sidewall panels, are built as a sandwich construction with glass fiber reinforced face sheet and honeycomb cores. For thermal and acoustic insulation purposes, glass wool packages are attached on their backside. This design comes with many advantages such as high weight specific mechanical properties and excellent fire retardancy. However, curing of thermoset resins leads to long cycle times during manufacturing and limited options for repair in case of damage or recycling at the end of product life. To overcome these challenges, a new hot press process has been developed to transform thermoplastic foams into structural foams. [1–3]

Thermoplastic foams allow manufacturing of low-weight parts with densities as low as 3 % of the polymer density. They are available in a wide range of polymers, such as polyetherimide (PEI) with excellent flame retardancy and certification according to FAR 25.853 [4, 5]. Thermoforming these foams allows part manufacturing with low cycle times. However, due to reduced densities, they show low mechanical properties.

Thermoplastic structural foams have a sandwich-like structure with a dense surface and a porous core and show higher mechanical properties compared to foam parts as well as lower part weights compared to solid parts. The majority of reported approaches to create thermoplastic structural foams are using foaming techniques in injection molding processes. [6–10]. However, they are manufactured to final part geometry in reaction injection molding processes and reduction of part densities lower than 75 % compared to solid parts is increasingly difficult. [11]

Polymer foams made from amorphous thermoplastic material show compression behavior that highly depends on process temperature. This behavior can be used to transform thermoplastic foams into structural foams through localized compaction of foam cells. This paper presents a hot press process to transform thermoplastic foams into structural foams. Behavior of SABIC ULTEM XP foam in this described process and influence of transformation into structural foams on the bending properties and charpy impact strength is discussed. First results of the transformation of thermoplastic foams into structural foams by using a variothermal hot press process have been presented at 5th ITHEC [12]. Results for structural foams manufactured with Diab Divinycell F40 and F50 will be presented at Sampe Europe Conference 21 [13].

2. THERMOPLASTIC FOAMS

Cellular materials with a three dimensional structure are called foams. If the solid material is only contained in the cell edges and struts, the foam can be classified as an open cell foam. Many materials can be foamed, with polymers being the most common. Relative density provides the most important property of a polymer foam: [14, 15]

$$\phi = \frac{\rho_f}{\rho_s} \tag{1}$$

Here, ρ_f is the density of the foam and ρ_s the density of the solid material. For mechanical properties of polymer foams, a power law relationship is applicable in most cases: [15]

$$\frac{X_f}{X_s} = \phi^n \tag{2}$$

X_f represents the foam property and X_S the property of the solid material. Values of the exponent n usually lie between $1.0 < n < 2.0$. If $n = 1$, this relation represents the rule of linear mixture. Based on a review in literature, Gibson and Ashby reported, that the correlation between relative modulus and relative density of open cell foams can be formulated as [14, 15]:

$$\frac{E_{Cf}}{E_s} = \left(\frac{\rho_f}{\rho_s}\right)^2 \tag{3}$$

doi: 10.25967/550106

2.1. Compression Behavior of Foams

Stress-strain curves of thermoplastic foams determined in compression tests can be divided into three distinct sections: Elastic and plastic deformation and a final stage called densification. Transition from elastic to plastic deformation can be determined by identifying yield strength, a local maximum in compression stress. Yield strength represents the pressure that cellular material can withstand before cell struts and walls begin to break or buckle. Plastic deformation during compression tests can be observed as a constant level of stress with increasing strain. Densification is then caused by an increasing amount of opposing cell walls crushed together, leading to an exponential rise in compression stress. Compression stress in thermoplastic foams strongly depends on the process temperature and the glass transition temperature of the polymer (see Figure 1). With increasing process temperature, yield strength as a local stress maximum moves to lower strain values. At the same time, stress levels necessary to cause plastic deformation are reduced. When the process temperature is increased above glass transition temperature, yield strength can no longer be detected. We can also observe, that the onset of densification moves to higher strain values, allowing to compact foam cells further without drastic increase in compression stress.

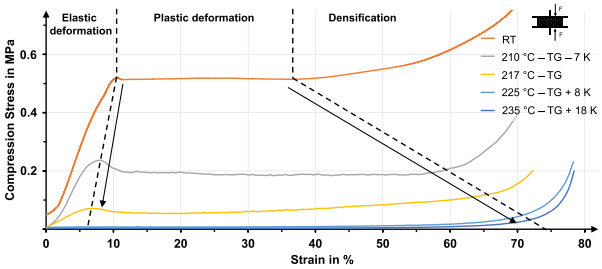

Figure 1: Stress-strain curves of thermoplastic foam at different temperatures

2.2. Manufacturing of Polymer Skin by Compacting Foam Cells

This temperature dependent behavior can be used to transform thermoplastic foams into structural foams by applying localized compaction of foam cells for producing polymer skins. The compaction s can be calculated as follows:

$$s = d_i - d_{i+1} \tag{4}$$

Here, d_i is the part thickness before and d_{i+1} the part thickness after the process. During compaction the part thickness is reduced, but part density is increased. When compaction is only applied locally, it is possible to to create a density gradient over the part cross section. To produce structural foams with such a density gradient, the aim should be to achieve polymer density in the area of compacted foam cells.

The thickness t_{theo} of this polymer skin can be calculated by using a linear relation between compaction s and the foams relative density Φ:

$$t_{theo} = s * \frac{\rho_f}{\rho_s} \tag{5}$$

By using this relation, it can be assed, how far foam cells in the skin area have been compacted and estimate the density.

3. PROCESS AND MATERIALS

An isochorous and isothermal hot press process has been developed to transform thermoplastic foams into structural foams, (see Figure 2). In this process, only one tool is heated to temperatures above glass transition temperature of the polymer to compact foam cells only locally and prevent a complete collapse of the foam. The bottom tool half remains at room temperature. To create a sandwich structure and produce polymer skins on both surfaces of the foam, two process steps are necessary. To apply equal compaction in both process steps, the minimal height of the cavity between both tool halves is limited using steel strips.

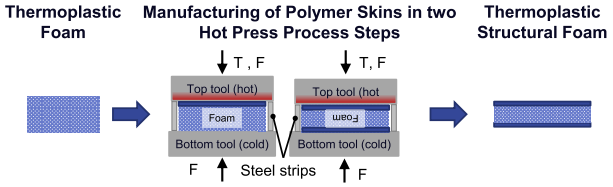

Figure 2: Hot press process for manufacturing structural foams

The transformation of two PEI foams (Sabic Ultem Foam XP50 and XP110) into structural foams was investigated. An overview of the most important properties of both foams can be found in Tab.1. Glass transition temperature T_G of PEI is at 217 °C [16]. To calculate relative properties of structural foams - such as relative densities and relative bending properties - the measured properties were compared to reported properites of standard PEI injection molding material ULTEM RESIN 1000 [16].

TAB 1. Properties of XP50 and XP110 [4, 5]

	Density	Initial thickness	Compressive strength
XP50	50 kg /m³	5.2 mm	0.5 MPa
XP110	110 kg/m³	4.9 mm	1.7 MPa

Structural foams were manufactured at tool temperatures of 225 °C and 235 °C, 8 K and 18 K above T_G. Process pressure was set below compressive strength of the foam at room temperature and was held for 180 seconds. Structural foams with polymer skins on both foam surfaces were produced with thicknesses of 4 mm, 3 mm and 2 mm through equal compaction s in two process steps. With part thicknesses being d_0 (semi-finished product), d_1 (after the first process step with one polymer skin) and d_2 (after the second process step with two polymer skins) – (see Figure 3).

Figure 3: Relation between part thickness and compaction

As mentioned before, compaction can be calculated using equation (4). Compaction in both process steps was equal:

(6) $$s = d_0 - d_1 = d_1 - d_2$$

Five structural foams with a size of 100 x 100 mm² have been produced for every part thickness and material.

4. METHODS OF ANALYSIS

Optical analysis of microsections cuts from these foams allowed quantifying the produced skin thicknesses and mechanical testing of these materials allowed assessing the change in bending properties and charpy impact strength.

4.1. Optical Analysis of Structural Foam

To determine the impact of process parameters on production of polymer skin, five structural foams per parameter set with polymer skins on both sides were manufactured. For further analysis of the structure one microsection per structural plate was cutout and prepared. These microsections with a width of 20 mm were then divided into 5 individual sections for the determination of average skin thickness. The polymer skins created in this process can be analysed by using microsections cuts from the structural foam. Here, it is easy to distinguish between the white higher density polymer skin area and the dark low density foam core. The polymer skin is created by compacting foam cells. This compaction is supported by foam structure leading to an uneven formation on the core side (see Figure 4).

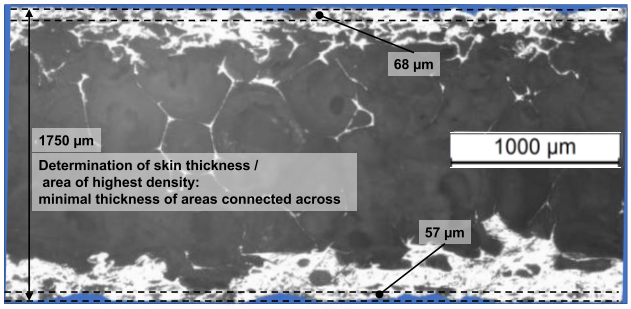

Figure 4: Analysis of manufactured polymer skin

The result of this process is a polymer skin at the surface of the foam with increased density compared to the foam core. To determine the density of this skin area and connect it to the applied compaction, the minimal thickness of the connected polymer areas was measured by using two parallel bars. The first bar was placed on the surface of the sample, while the second bar was placed towards the core side. The second bar had to be supported by many points across the width of the section. Mean values and standard deviations have been determined using the skin thickness of each of these individual sections. Using these values, it is possible to compare the applied compaction of foam cells with the theoretical skin thickness, that will be achieved, if the material density is increased from foam to polymer density. Through this approach, the effect of the applied process parameters on the compaction of foam cells and density increase in this skin area can be assessed.

4.2. Mechanical Testing of Structural Foam

The impact of the transformation into structural foams on mechanical properties was examined in three point bending tests and charpy impact tests, conducted according to DIN EN ISO 178 and 179. Test specimen were cut to length of 80 mm and width of 10 mm. For three point bending tests (see Figure 5) the support width L was set to:

(6) L=(16*d)±1

Here, d is the part thickness.

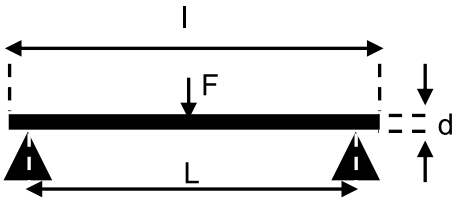

Figure 5: Schematic for three point bending test according to DIN EN ISO 178 [17]

Bending modulus in this test procedure is determined as the secant gradient between strain of 0.05 % and 0.25% [17]:

(7) $$E_f = \frac{\sigma_{f-0.25\%} - \sigma_{f-0.05\%}}{0.25\% - 0.05\%}$$

Bending strength is the maximum bending stress during the test.
For charpy impact tests the support width L was set to 62 mm (see Figure 6). Specimen were tested using flatwise impact by using a 4 Joule hammer.

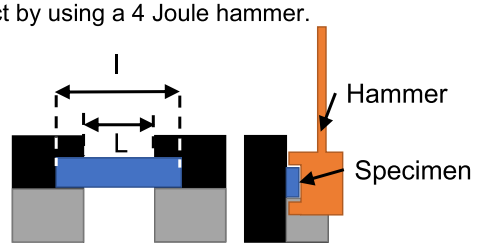

Figure 6: Schematic for flatwise charpy impact test according to DIN EN ISO 179 [18]

Impact strength was calculated as the ratio of energy loss to the area of the cross section [18]:

(8) $$a_{cU} = \frac{E_c}{h * b} * 10^3$$

5. RESULTS

Figure 7 shows the measured skin thickness plotted over the compaction that was applied to manufacture the polymer skin. At first glance, a clear correlation between compaction and polymer skin could not be identified. Measured skin thicknesses seem to be at an equal level, independent of compaction. An increase in tool temperature appears to have an impact on a thicker area from the surface with an average of 118 µm at 225 °C and 128 µm at 235 °C. However, if the measured skin thicknesses are compared to the theoretical values, it can be assessed, how far foam cells were compacted. The dotted lines in this plot represent this theoretical relation between compaction and skin formation for XP50 and XP110. The theoretical skin thickness is achieved, when foam cells are completely compacted and polymer density is reached. Especially for small compactions, the measured skin thickness is much higher than its theoretical counterpart. With increasing compaction, this difference appears to decrease.

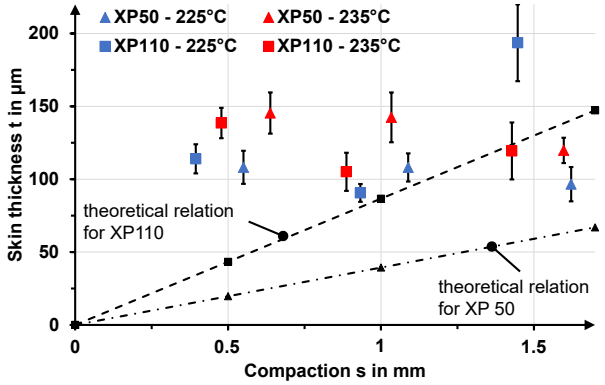

Figure 7: Comparison of theoretical and measured skin thickness

As mentioned before, the density in the measured polymer skin can be approximated, if the theoretical skin thickness is divided by the measured skin thickness.

$$\phi_{Skin} = \frac{\rho_{skin}}{\rho_{polymer}} = \frac{t_{theo}}{t_{measured}} \quad (9)$$

Figure 8 shows this relative density of the skin area over the compaction that was applied during manufacturing. This comparison reveals, that it is possible to achieve higher density in the skin area, if apply higher compactions are applied to the material. For compactions of 0.5 mm, it was possible to achieve relative densities between 20 % and 30 % in the polymer skin area.

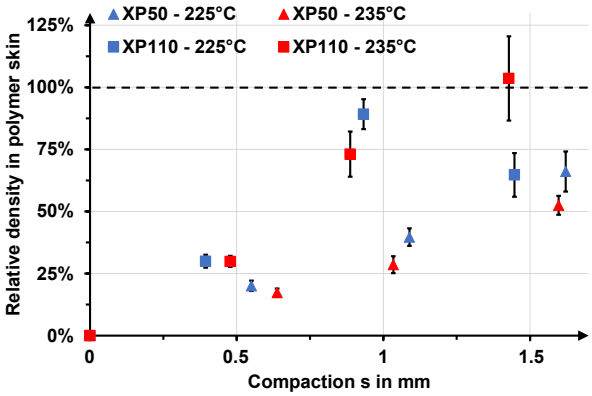

Figure 8: Estimated density in manufactured polymer skins

For optimization of the process, it should be examined, whether it is possible to further increase density for small compactions.

Three point bending tests (see Figure 9) showed an increase in bending modulus of more than 10 times with increasing compaction for both materials. Bending modulus in XP50 increased from 0.02 GPa up to 0.22 GPa. Bending modulus in XP110 increased from 0.05 to 0.6 GPa. The course of this increase, especially in structural foams made from XP110, is progressive. In addition, this increase for structural foams produced at 235 °C is higher than for structural foams produced at 225°C.

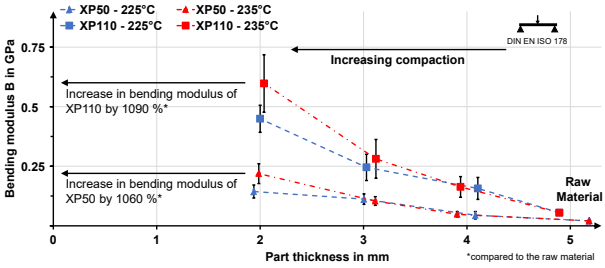

Figure 9: Bending modulus of foam parts with different thicknesses

Figure 10 depicts in a similar manner that bending strength in these structural foams increases 7 times in XP110 from 3.3 MPa to 23 MPa and 8 times in XP50 from 0.8 MPa to 6.5 MPa. Here, a higher increase in bending strength can be observed with increasing temperature, especially in parts made with XP110.

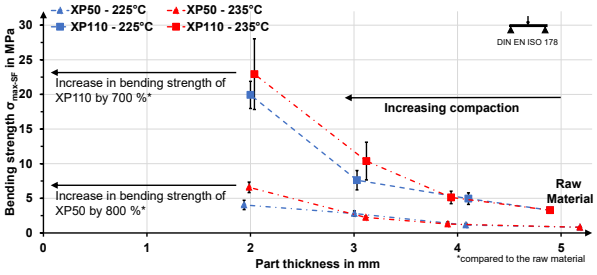

Figure 10: Bending strength of foam parts with different thicknesses

To further investigate this increase in bending modulus, the relative bending modulus can be plotted over the relative part density. The relative bending modulus and density are the measured properties in relation to the solid polymer. This allows a better representation of their correlation. The plot shows two power-law relations as boundaries enclosing the measured values, with n = 1 being the upper boundary and n = 2 being the lower boundary. Using the power-law relation with n = 1.35, it is possible to approximate the measured bending modulus within an acceptable range. However, with increasing relative densities the exponent in the power law relation seems to decrease.

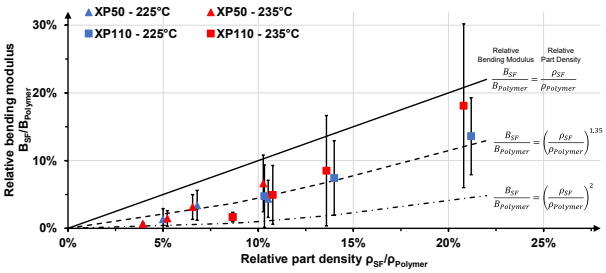

Figure 11: Relation between relative bending modulus and relative density of structural foams

In Figure 12 the relative bending strength is plotted over the relative part density. Again, the course of the power-law relation with n = 1 and n = 2 enclose the measured values. However, this time a power-law relation with n = 1.5 can be applied to approximate the measured values.

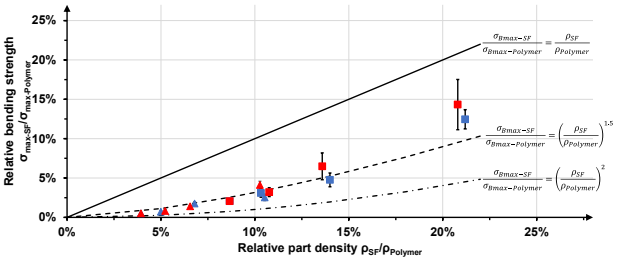

Figure 12: Relation between relative bending strength and relative density of structural foams

The last mechanical property to look at is charpy impact strength (see Figure 13). Compared to the raw material, charpy impact strength in XP50 increased by 2.3 times from 0.65 to 1.5 kJ/m² and in XP110 by 1.4 times from 3.8 to 5.4 kJ/m².

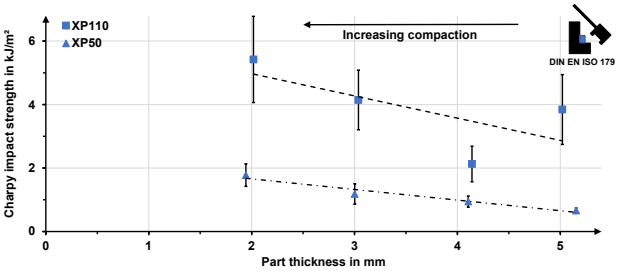

Figure 13: Charpy impact strength of structural foam

As shown in Figure 14, charpy impact strength also depends on part density. However, with structural foams it is possible to achieve equal impact strengths compared to the solid polymer, with relative densities being as low as 15% due to the porous structure of the foam core.

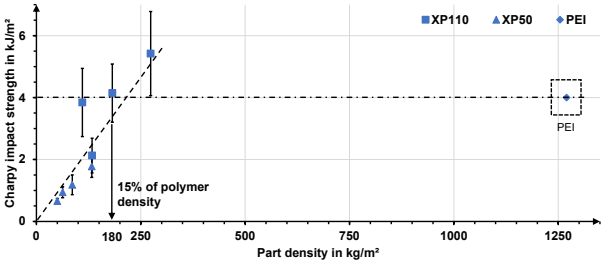

Figure 14: Relation between density and charpy impact strength of structural foam

6. CONCLUSION AND OUTLOOK

Thermoplastic foams allow production of low weight parts, but they also have low mechanical properties. Thermoplastic foams can be transformed into structural foams by using hot press processes. Polymer skins - manufactured in these processes - can be analyzed using optical methods to quantify their thicknesses and evaluate the density increase. The mechanical properties of the thermoplastic foams and the structural foams were determined in three point bending tests and charpy impact tests. It was shown, that mechanical properties can be increased without changing the part weight by transforming thermoplastic foams into structural foams by applying hot press processes. The increase in bending modulus and strength can be approximated using the relative part density in a power-law relation. The increase in charpy impact strength can be linked to the increase in density as well. With these structural foams impact strengths of the solid polymer can be reached at a fraction of its density.
As an outlook, promising topics relating to manufacturing structural foams by using hot press processes are presented in Figure 15 and Figure 16. By applying the presented approach, it should be possible to produce structural foam parts with specific geometries and local differences in part and skin thickness.

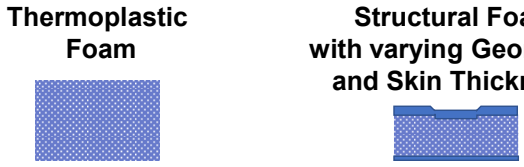

Figure 15: Schematic for structural foam with varying geometry and skin thickness

Flat structural foam parts can be produced by using continuous compression molding processes to increase production efficiency. These flat parts can also be transformed into a final part geometry by applying thermoforming processes.

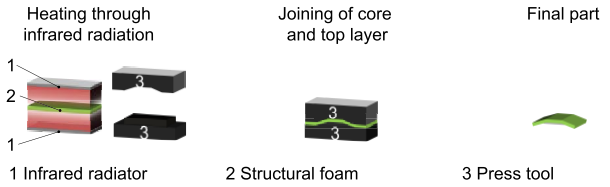

Figure 16: Schematic for thermoforming of flat structural foam into final part geometry

Another promising objective is developing a support tool to predict mechanical properties of structural foam for application specific selection of semi-finished thermoplastic foam.

7. ACKNOWLEDGEMENT

This study has been conducted in the frame of the research project “Sophia – Smart processes and optimized designs for high production cadences” funded by the Federal Ministry of Economic Affairs and Energy (BMWi) on the basis of a decision by the German Bundestag (funding reference 20X1715D).

8. REFERENCES

[1] N. R. C. Staff and C. o. F. a. S.-R. M. f. C. T. "Aircraft, Improved Fire- and Smoke-Resistant Materials for Commercial Aircraft Interiors: *A Proceedings*." Washington, 1995.

[2] S. Black, "Advanced materials for aircraft interiors: *Applications aren't as demanding as airframe composites, but requirements are stil exacting - passenger safety is key*." Compositesworld.com, 2006.

[3] M. Barile *et al.,* “Thermoplastic Composites for Aerospace Applications,” in *Revolutionizing Aircraft Materials and Processes*, S. Pantelakis and K. Tserpes, Eds., Cham: Springer International Publishing, 2020, pp. 87–114; 978-3-030-35345-2.

[4] Sabic, “ULTEM™ Foam_XP050: Technical Data Sheet,” 2018.

[5] Sabic, “ULTEM™ Foam_XP110: Technical Data Sheet,” 2018.

[6] J. L. Throne and R. G. Griskey, “Structural thermoplastic foam? A low energy processed material,” *Polym Eng Sci*, no. 10, 1975, pp. 747–756, doi: 10.1002/pen.760151007.

[7] S. Y. Hobbs, “Predicting the Flexural Rigidity of Thermoplastic Structural Foams,” 1976.

[8] V. Kumar and J. E. Weller, “A model for the unfoamed skin on microcellular foams,” 1994.

[9] S. Djoumaliisky *et al.,* “Structure of PP Structural foam Moldings Made by the Gas-Counterpressure Process,” no. 2, 1997, pp. 257–271, doi: 10.1080/03602559708000618.

[10] H. Eckardt and K. Alex, “Structural and coinjection foam molding,” *Adv. Polym. Technol.*, no. 2, 1981, pp. 40–49, doi: 10.1002/adv.1981.060010207.

[11] J. Pinto *et al.,* “A novel route to produce structural polymer foams with a controlled solid skin-porous core structure based on gas diffusion mechanisms,” *Jnl of Sandwich Structures & Materials*, no. 3, 2020, pp. 822–832, doi: 10.1177/1099636218777434.

[12] M. Salmins and P. Mitschang, "Density Influence on the formation of skin layers in integral sandwich structures based on open porous pesu foams." 5th International Conference and Exhibition on Thermoplastic Composites, 2020.

[13] M. Salmins and P. Mitschang, "Manufacturing of lightweight sandwich foam with optimized bending properties in a hot press process." Sampe Europe Conference 21 Baden/Zurich, 2021.

[14] L. J. Gibson and M. F. Ashby, "Cellular solids: *Structure and properties*." Cambridge: Cambridge University Press, 1997, doi: 10.1017/CBO9781139878326; 0-521-49911-9.

[15] N. C. Hilyard and A. Cunningham, "Low density cellular plastics: *Physical basis of behaviour,"* 1st ed. London: Chapman & Hall, 1994; 0-412-58410-7.

[16] Sabic, "ULTEM™ Resin 1000". Technical Data Sheet, 2021.

[17] DIN EN ISO 178 : Bestimmung der Biegeeigenschaften, 178, 2013.

[18] DIN EN ISO 179-1: Bestimmung der Charpy-Schlageigenschaften, 179-1, 2010.